

UNDERSTANDING AND OBSERVING THE $H\alpha$ CHROMOSPHERE

Rob Rutten

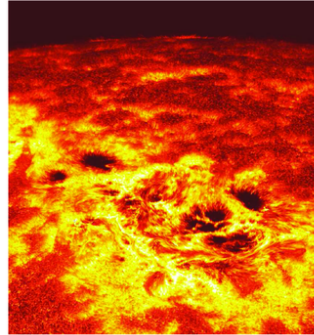
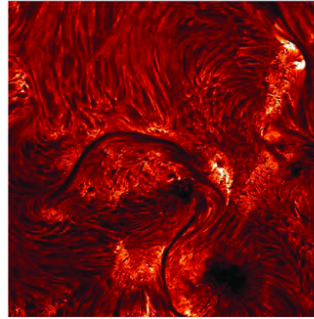
Lingezicht Astrophysics Deil & Institutt for Teoretisk Astrofysikk Oslo

http://www.staff.science.uu.nl/~rutte101/Graphical_Introduction.html

Chromosphere at eclipse

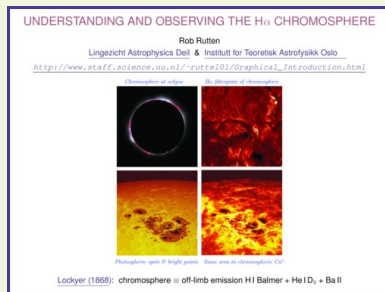


$H\alpha$ filtergram of chromosphere



Photospheric spots & bright points Same area in chromospheric Ca^{II}

Lockyer (1868): chromosphere \equiv off-limb emission H I Balmer + He I D_3 + Ba II



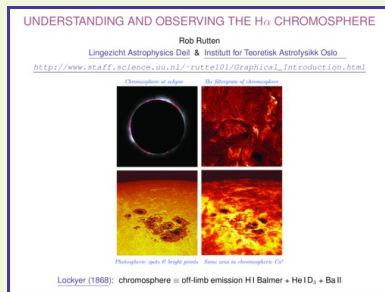
Format: in this webpost I added tinted pages after each talk display that emulate my oral explanation (or rather, what I wanted to say but didn't because of the time limit). I also replaced movie-opening clickers by weblinks to download them, and turned citations into weblinks that should open the corresponding ADS page in your browser.

Navigation: clicking on the display title or insert thumbnail returns you to where you came from. Each talk display also has a hidden clicker top-left returning you to the first display, and one at top-right to a thumbnail index. These are explicit in the tinted insert pages, as here.

Title: this talk is mostly about understanding the formation of $H\alpha$, with a plea for $H\alpha$ observing for IRIS at the end.

My affiliation: I spent fifty years in [solar physics at Utrecht](#) but since early 2012 all [Utrecht astronomy is gone](#). Dutch solar physics vanished with it. Fortunately, I am still welcome at Oslo.

[Graphical introduction to NLTE chromospheric line formation](#): a similarly expanded posting of a brief tutorial that I gave at the SDO-4/IRIS/Hinode Workshop in Monterey earlier this year. It covers the same $H\alpha$ results but adds an extended didactic introduction to scattering in the solar atmosphere.



The above image quartet adorned the decadal-survey White Paper by [Ayres et al. \(2009\)](#). The first image illustrates the naming of the chromosphere by [Lockyer \(1868\)](#) (I typed the report into ADS). Using a new spectroscope he found a pink ring around the Sun, also outside prominences, dominated by a few Fraunhofer lines later identified as $H\alpha$, $H\beta$, He I D₃, and Ba II. By definition the chromosphere is whatever emits these lines, making $H\alpha$ the quintessential chromosphere diagnostic. Ca II 8542 Å comes closest.

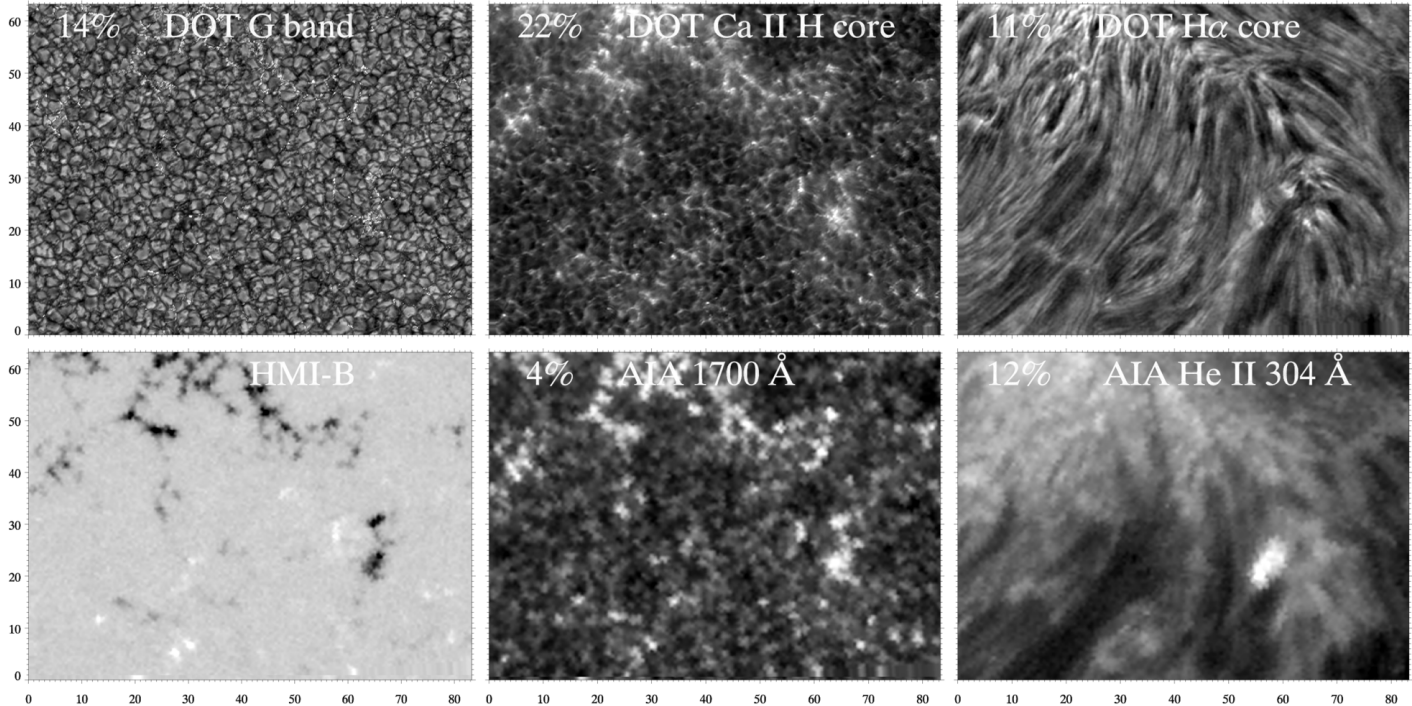
The second image, from the [DOT](#), shows the $H\alpha$ chromosphere on the disk. It is a dense mass of fibrils wherever there is a bit of activity. It is not clear whether these fibrils are cylindrical fluxtubes, ridge-shape $\tau = 1$ corrugations, sheets, or sheet warps resembling curtain folds. They seem to outline horizontal field topography. Vertical fields are less easily seen in $H\alpha$ but are of larger interest to coronal mass and energy loading (see [Rutten 2012](#) for an overview).

The lower-left DOT image shows the photosphere in the G band. Its bright points mark strong-field footpoints, without sign. Signed magnetograms from MDI and HMI are habitually used for field topography mapping. Since it becomes force-free only above the chromosphere, $H\alpha$ fibril patterns cannot be predicted this way. They should be monitored SDO-like and constrain NLFFF extrapolation.

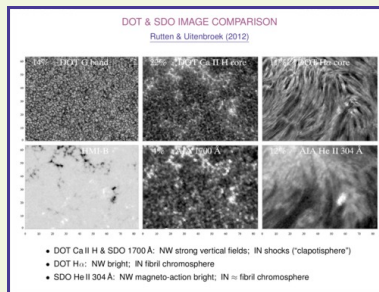
The lower-right DOT image is corresponding wide-band Ca II H. It shows chromospheric emission where it is bright, elsewhere cool shock-ridden gas underneath the fibril chromosphere.

DOT & SDO IMAGE COMPARISON

Rutten & Uitenbroek (2012)



- DOT Ca II H & SDO 1700 Å: NW strong vertical fields; IN shocks (“clapotisphere”)
- DOT H α : NW bright; IN fibril chromosphere
- SDO He II 304 Å: NW magneto-action bright; IN \approx fibril chromosphere



A more detailed scene comparison for an area with plage (upper part of the field of view) and quiet network and internetwork (lower part). Upper row: images from the [DOT](#). Lower row: images from [SDO](#). The percentage numbers specify the relative rms brightness contrast per image. Solar images are usually byte-scaled for maximum display contrast; the actual contrasts are often much lower.

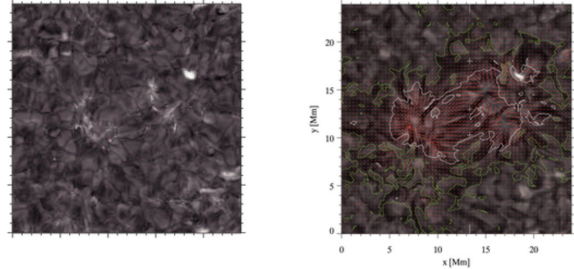
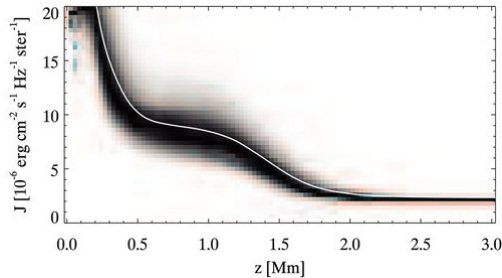
First column: photosphere. The principal ingredients are the granulation and strong-field magnetic concentrations, with p -mode modulation evident in time-sequence sampling. Zooming in on the G-band bright points shows their close correspondence with (unsigned) HMI field concentrations.

Second column: bright chromosphere in plage and network but shock-ridden "clapotisphere" elsewhere. The latter gas, underneath the $H\alpha$ fibrils, isn't chromosphere because it does not radiate $H\alpha$. The Ca II H and 1700 Å scenes are closely similar, apart from obvious difference in sharpness. The rms contrasts differ much because such wide-band Ca II H is dominated by near-LTE inner-wing brightness, 1700 Å by bound-free scattering.

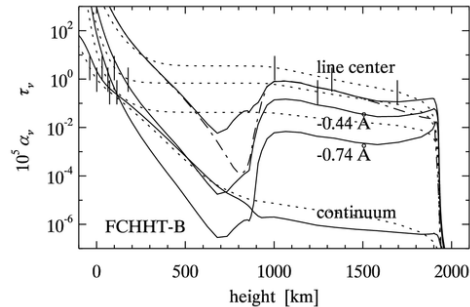
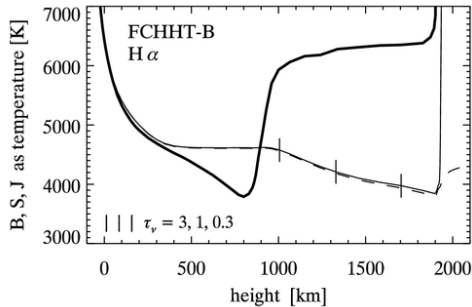
Third column: chromosphere. Both $H\alpha$ and He II 304 Å show bright grains at fibril footpoints near magnetic concentrations and darker fibrils covering the internetwork, with some but not 1:1 similarity between the two diagnostics. He II 304 Å is supposed to sample the transition region. The rough similarity suggests that the latter shares the fibrilar morphology of the chromosphere. However, the bright blob seems specific for He II 304 Å.

RECENT RESULTS ON $H\alpha$ FORMATION

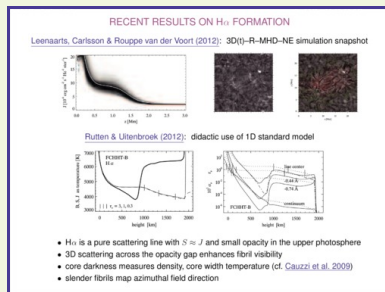
Leenaarts, Carlsson & Rouppe van der Voort (2012): 3D(t)–R–MHD–NE simulation snapshot



Rutten & Uitenbroek (2012): didactic use of 1D standard model



- $H\alpha$ is a pure scattering line with $S \approx J$ and small opacity in the upper photosphere
- 3D scattering across the opacity gap enhances fibril visibility
- core darkness measures density, core width temperature (cf. [Cauzzi et al. 2009](#))
- slender fibrils map azimuthal field direction

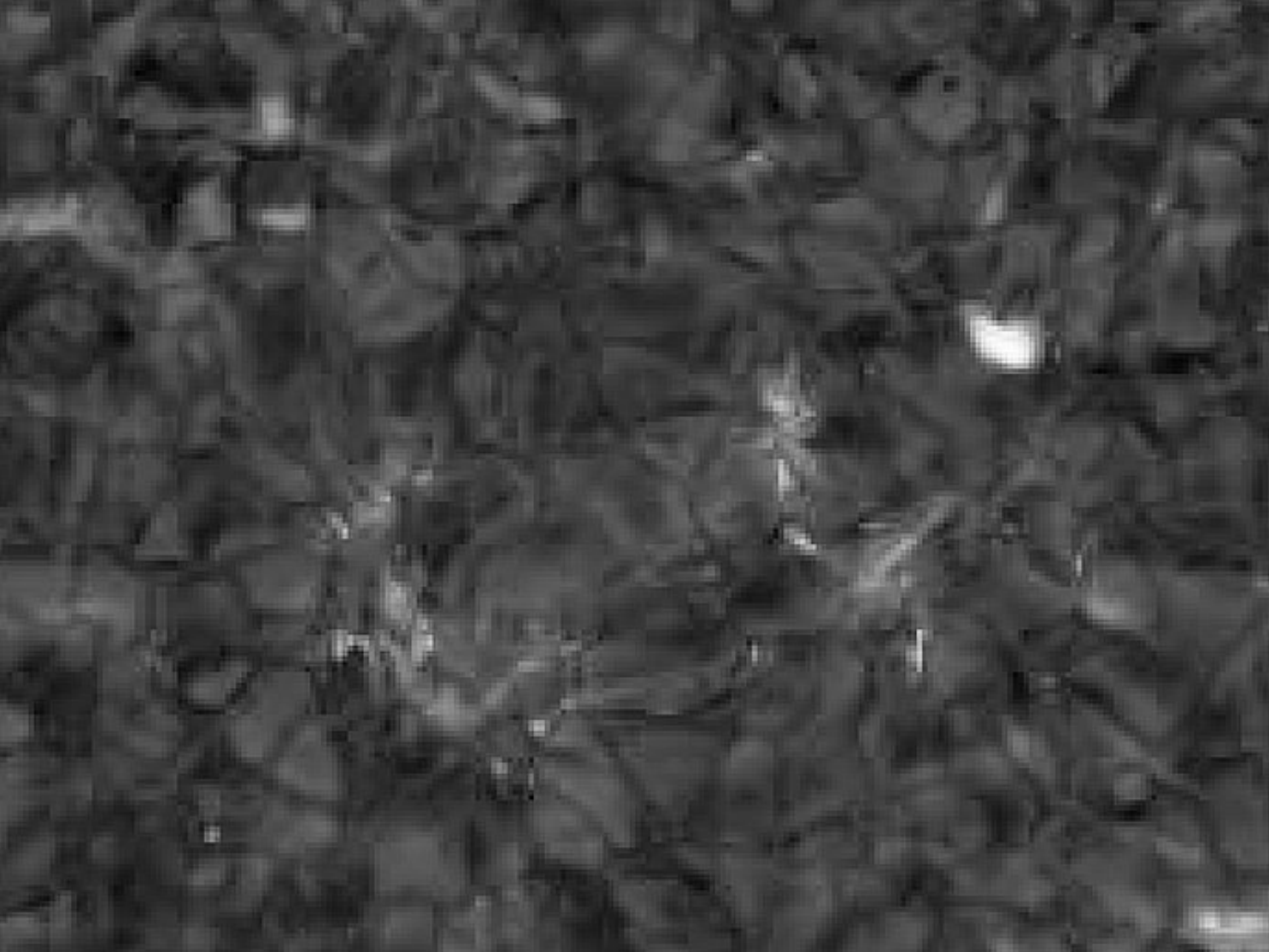


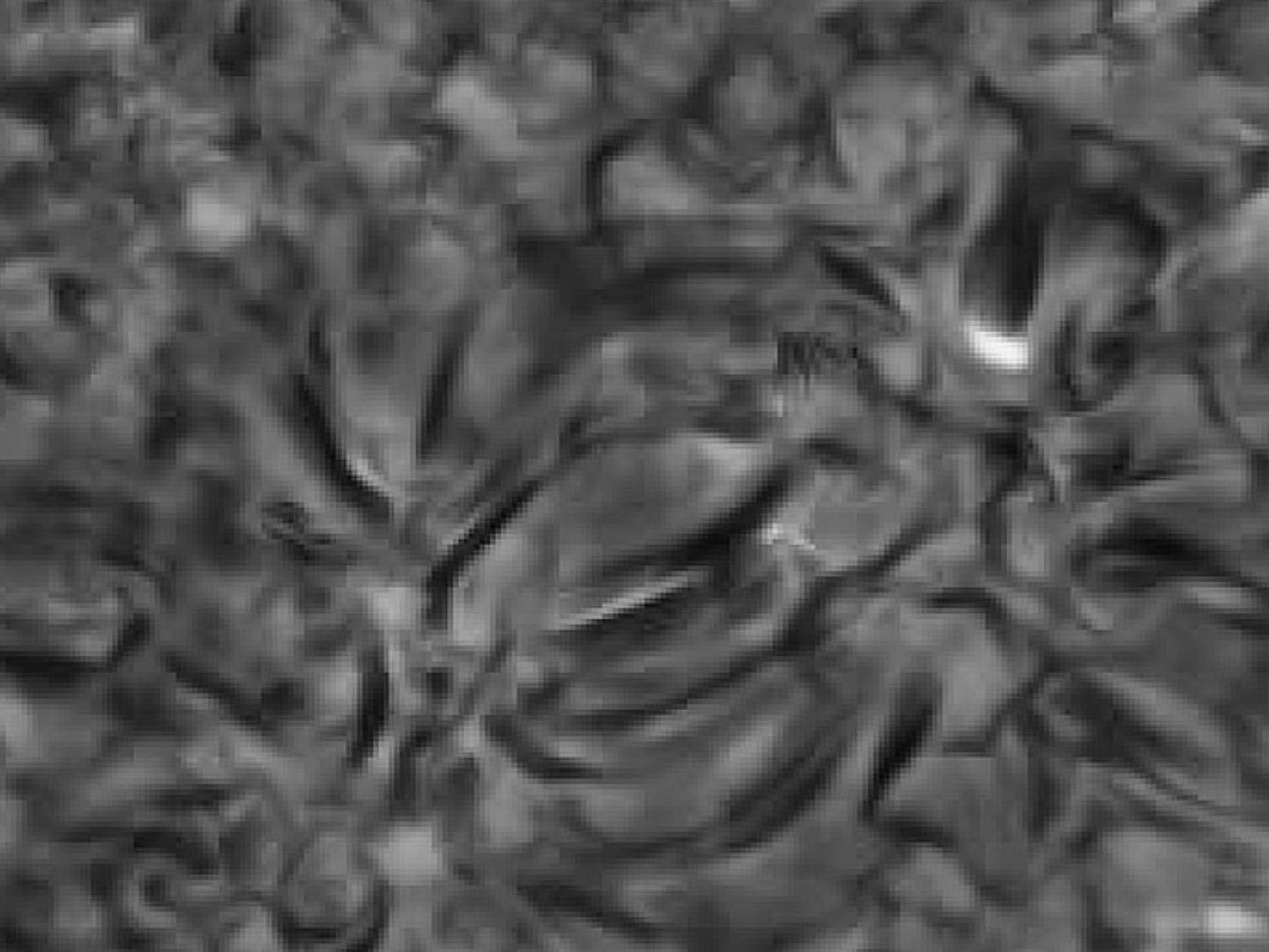
These two papers are complementary. [Leenaarts et al. \(2012\)](#) analyze $H\alpha$ formation in a snapshot from a 3D time-dependent MHD simulation (including non-equilibrium hydrogen ionization) with the Bifrost code. [Rutten & Uitenbroek \(2012\)](#) analyze $H\alpha$ formation in the most recent 1D static plane-parallel hydrostatic-equilibrium standard model, FCHHT-B of [Fontenla et al. \(2009\)](#).

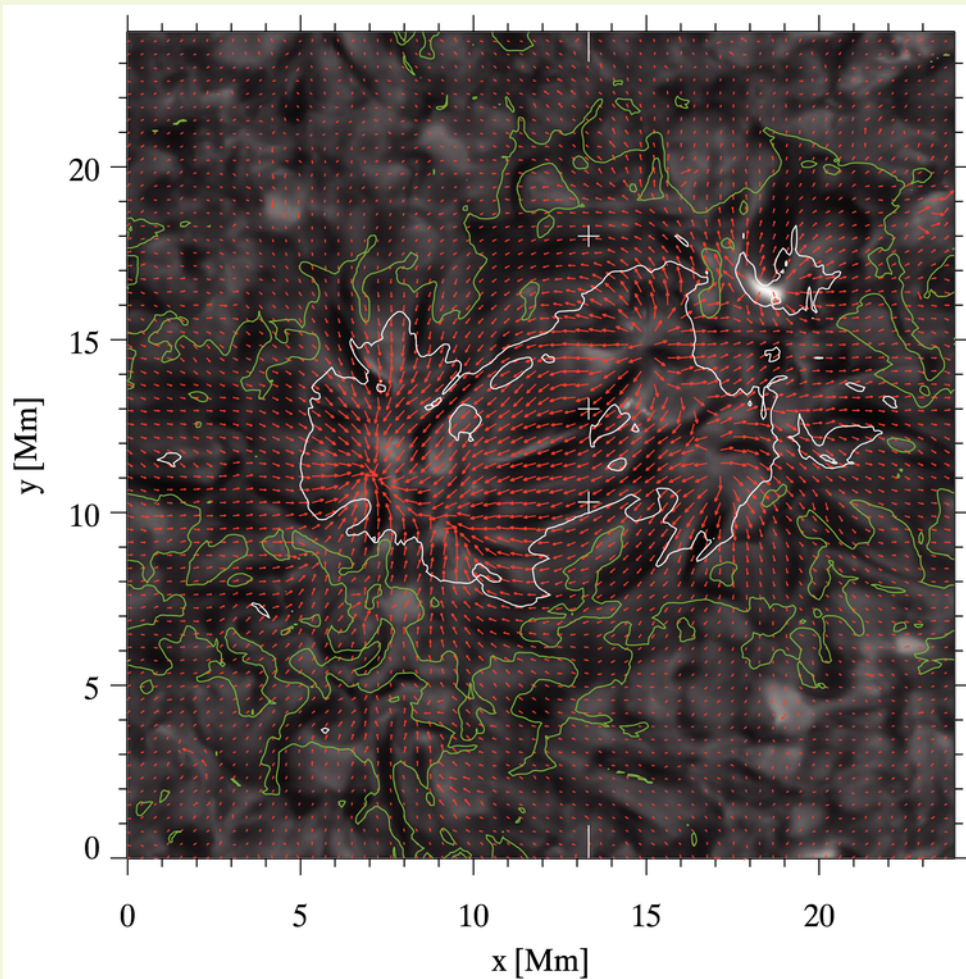
The key result is that $H\alpha$ is a resonant scattering line. Its line source function S is given by the angular mean of the radiation field J everywhere above the deep photosphere. There is a high- J plateau across the cool upper photosphere fed by scattering from below and from above. It is due to low line opacity, as shown by the last graph for line-center and inner-wing wavelengths. The optical depth buildup (dotted) is negligible across this opacity gap. Above it, S has an outward drop akin to the $\sqrt{\epsilon}$ drop in a scattering isothermal atmosphere, with Eddington-Barbier emergent-intensity sampling. Large thermal broadening makes the core width a temperature diagnostic ([Cauzzi et al. 2009](#)).

The first image thumbnail is a clicker opening the next page, showing a cutout of the Bifrost image when the $H\alpha$ formation is computed along columns in 1D fashion. The next page has this done in 3D. Blink the two to see how strikingly the fibrils come into view in the 3D case. The underlying larger-contrast granulation pattern is washed out by 3D scattering across the opacity gap.

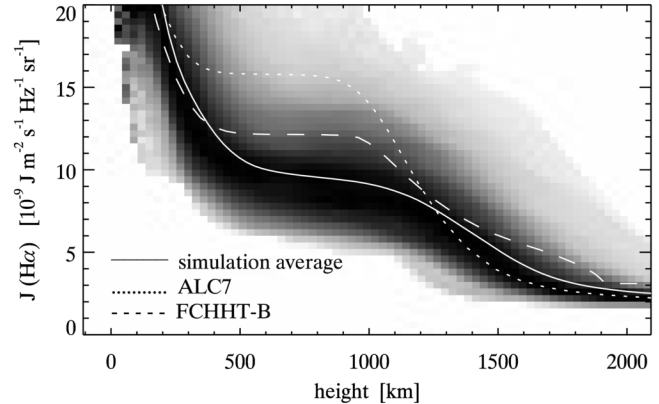
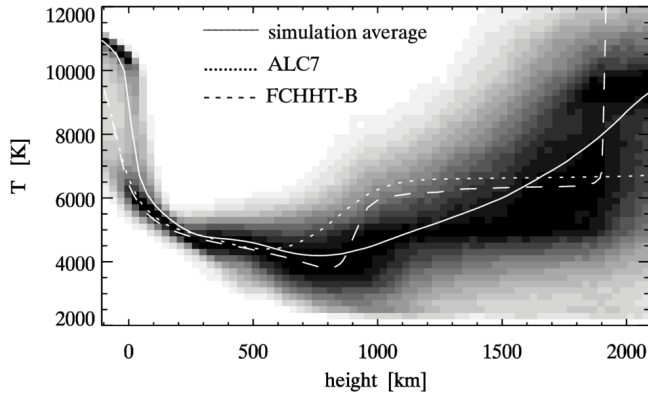
The second image thumbnail opens a page with figure 13 of [Leenaarts et al. \(2012\)](#). Blow it up to convince yourself that the fibrils roughly outline the azimuthal field direction (red arrows).



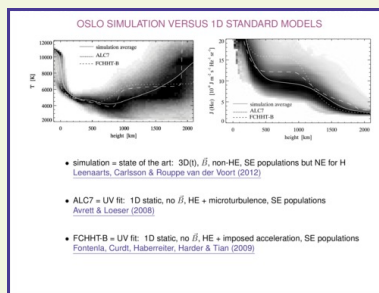




OSLO SIMULATION VERSUS 1D STANDARD MODELS



- simulation = state of the art: 3D(t), \vec{B} , non-HE, SE populations but NE for H
[Leenaarts, Carlsson & Rouppe van der Voort \(2012\)](#)
- ALC7 = UV fit: 1D static, no \vec{B} , HE + microturbulence, SE populations
[Avrett & Loeser \(2008\)](#)
- FCHHT-B = UV fit: 1D static, no \vec{B} , HE + imposed acceleration, SE populations
[Fontenla, Curdt, Haberreiter, Harder & Tian \(2009\)](#)



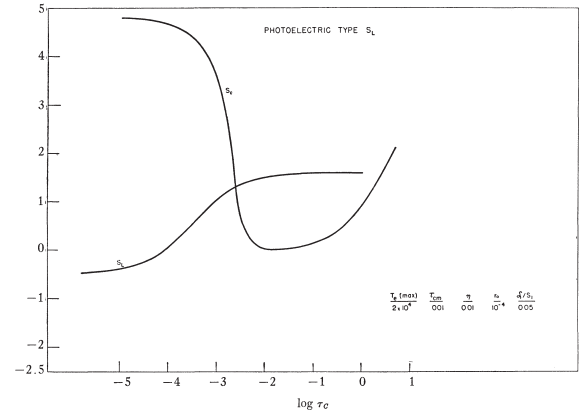
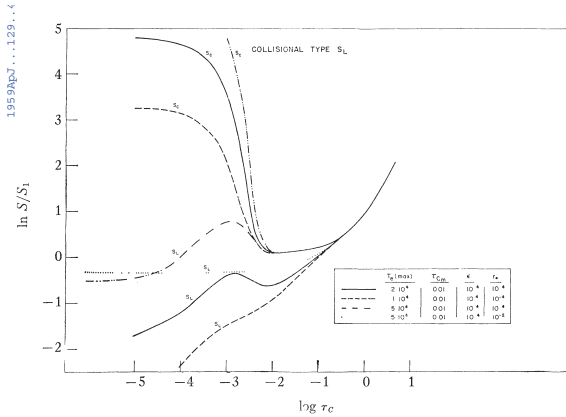
Comparison between the Oslo Bifrost simulation and the latest 1D standard models. The greyscale measures the occurrence probability per pixel across the simulation snapshot at the given height. Left: temperature against height. Right: mean intensity J at $H\alpha$ line center against height.

The bifurcation in simulation temperature in the deepest layers represents granules and intergranular lanes. The narrow neck in the upper-photosphere temperature, above reversed granulation and below the growth of acoustic waves into shocks, is close to 1D radiative-equilibrium models. However, the spread in $J(H\alpha)$ is already large.

The FCHHT-B chromosphere, supported by ad-hoc postulated acceleration, has isothermal-slab character. The deep temperature minimum below it boosts J across the corresponding $H\alpha$ opacity gap by strong backscattering from the slab. Higher up, the outward $S = J$ scattering decay of $H\alpha$ is similar for the three curves.

The T and $J(H\alpha)$ behaviors may seem arguably similar between the simulation and standard models. However, the conceptual differences between plane-parallel static hydrostatic-equilibrium modeling and the 3D(t) MHD simulation are enormous (cf. Newtonian gravitation versus general relativity). The $T(h)$ stratifications in the simulation vary tremendously, with shocks propagating upwards and sideways along fields and the increase to coronal temperature dancing rapidly up and down over a large height range. The standard models cannot be taken as spatio-temporal mean of these variations.

CANONICAL CHROMOSPHERIC LINE FORMATION



- CRD line source function including detour paths:

$$S_{\nu_0}^d = \frac{\bar{J}_{\nu_0} + \epsilon'_{\nu_0} B_{\nu_0}(T) + \eta'_{\nu_0} B_{\nu_0}(T_d)}{1 + \epsilon'_{\nu_0} + \eta'_{\nu_0}}$$

$$= (1 - \epsilon_{\nu_0} - \eta_{\nu_0}) \bar{J}_{\nu_0} + \epsilon_{\nu_0} B_{\nu_0}(T) + \eta_{\nu_0} B_{\nu_0}(T_d)$$

- ϵ = upper-lower collisional destruction fraction of total extinction

η = detour-path extinction fraction of total extinction

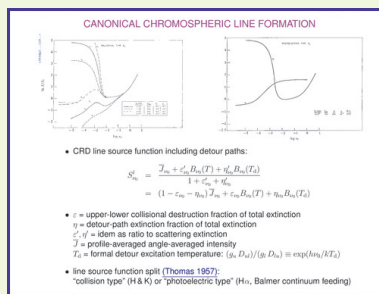
ϵ', η' = idem as ratio to scattering extinction

\bar{J} = profile-averaged angle-averaged intensity

T_d = formal detour excitation temperature: $(g_u D_{ul}) / (g_l D_{lu}) \equiv \exp(h\nu_0/kT_d)$

- line source function split ([Thomas 1957](#)):

“collision type” (H & K) or “photoelectric type” ($H\alpha$, Balmer continuum feeding)



Canonical wisdom. The graphs show the Planck function B and line source function S^l against optical depth (outward to the left). Both graphs are reprinted in both the [first \(1970\)](#) and [second \(1978\)](#) editions of Mihalas's "Stellar Atmospheres". [Jefferies & Thomas \(1959\)](#) produced them to illustrate the classification of [Thomas \(1957\)](#), splitting lines between "collision type" at left and "photoelectric type" at right. They named Ca II H & K an example of the first, H α an example of the latter.

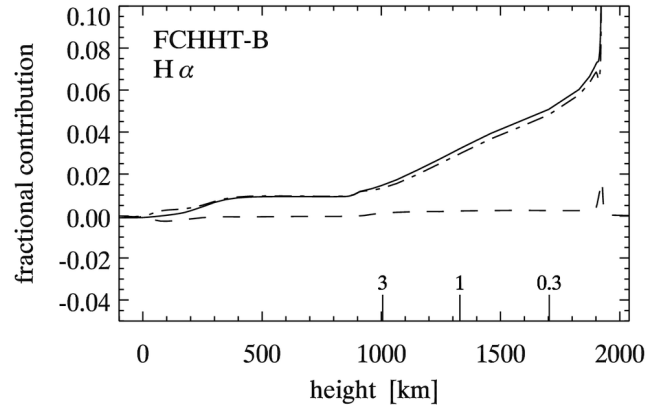
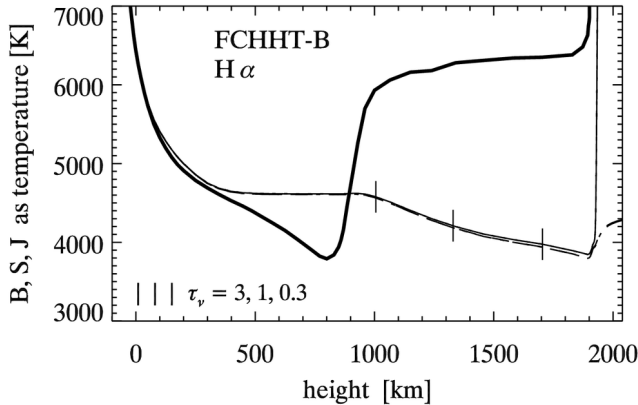
The difference was assigned to the ϵ/η ratio. For H α the high source function across the upper photosphere in the righthand graph was attributed to preponderance of detour-path $\eta B(T_d)$ contribution, for H α typically Balmer photoionization up from $n = 2$ plus cascade recombination (into high n followed by downward $\Delta n = 1$ steps) down into $n = 3$ and spontaneous H α emission.

The various curves in the lefthand graph match the source functions of Na I D1, Ca II 8542 Å, Ca II K, and Mg II k well (see my [Graphical introduction to NLTE chromospheric line formation](#)).

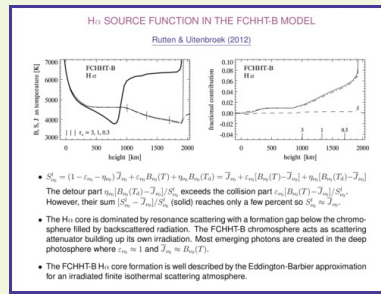
So is all well with the canonical wisdom? Not for H α ! In the simulation snapshot and in the standard models it is a scattering-dominated line just as the others, with negligible detour contribution except in the transition region. Its unusual superthermal upper-photosphere source function comes instead from chromospheric backscattering across its unusual opacity gap.

H α SOURCE FUNCTION IN THE FCHHT-B MODEL

Rutten & Uitenbroek (2012)



- $S_{\nu_0}^l = (1 - \varepsilon_{\nu_0} - \eta_{\nu_0}) \bar{J}_{\nu_0} + \varepsilon_{\nu_0} B_{\nu_0}(T) + \eta_{\nu_0} B_{\nu_0}(T_d) = \bar{J}_{\nu_0} + \varepsilon_{\nu_0} [B_{\nu_0}(T) - \bar{J}_{\nu_0}] + \eta_{\nu_0} [B_{\nu_0}(T_d) - \bar{J}_{\nu_0}]$
 The detour part $\eta_{\nu_0} [B_{\nu_0}(T_d) - \bar{J}_{\nu_0}] / S_{\nu_0}^l$ exceeds the collision part $\varepsilon_{\nu_0} [B_{\nu_0}(T) - \bar{J}_{\nu_0}] / S_{\nu_0}^l$.
 However, their sum $[S_{\nu_0}^l - \bar{J}_{\nu_0}] / S_{\nu_0}^l$ (solid) reaches only a few percent so $S_{\nu_0}^l \approx \bar{J}_{\nu_0}$.
- The H α core is dominated by resonance scattering with a formation gap below the chromosphere filled by backscattered radiation. The FCHHT-B chromosphere acts as scattering attenuator building up its own irradiation. Most emerging photons are created in the deep photosphere where $\varepsilon_{\nu_0} \approx 1$ and $\bar{J}_{\nu_0} \approx B_{\nu_0}(T)$.
- The FCHHT-B H α core formation is well described by the Eddington-Barbier approximation for an irradiated finite isothermal scattering atmosphere.



H α formation in the FCHHT-B model. This model is unlikely to describe any actual column in the solar atmosphere nor a spatio-temporal average, but it serves here for didactic breakdown.

Left: H α B, S, J with $S^{\text{total}} \approx S^l$ (thin solid) and $J \approx \bar{J}$ (dashed). Note that everywhere below the transition to the corona $S \approx J$, in particular in the $\tau = 0.3 - 3$ core formation range.

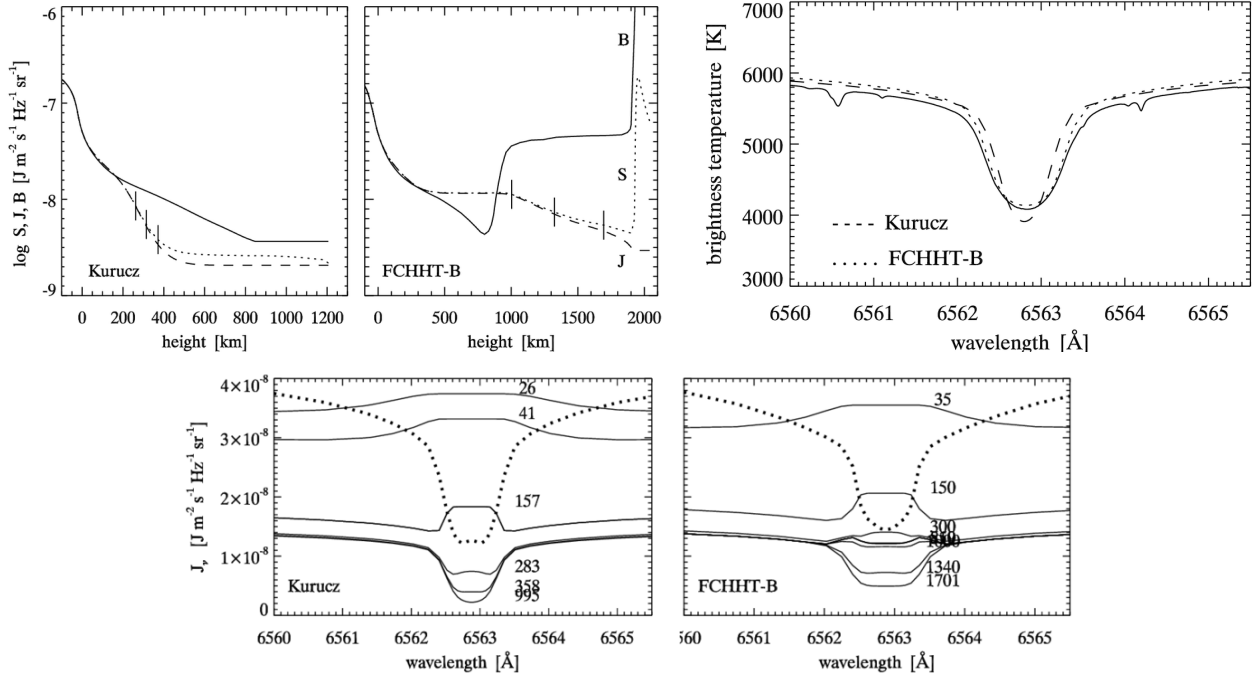
Right: fractional collisional (dashed) and detour (dot-dashed) contributions to S^l , as specified under the first bullet. The detour contribution becomes dominant in the transition to the corona, but that is transparent. Elsewhere $S \approx J$. Thus, H α is a scattering line. Most H α photons are created in the deep photosphere. Backscattering across the temperature-minimum opacity gap builds up J there.

Doubling the FCHHT-B chromospheric temperature produces appreciably higher $S \approx J$, peaking at 6000 K just above the gap, but also larger H α opacity so that $\tau = 1$ is reached already at 1300 km. This further-out sampling of the outward J decline compensates for the increase, so that $I(0,1) \approx S(\tau = 1)$ remains nearly the same. Doubling the chromospheric density produces only 200 K higher J across the gap, less elsewhere, but also moves $\tau = 1$ to about 1700 km and so lowers the emergent core intensity appreciably. Upshot: the core intensity is a density rather than a temperature diagnostic.

The height extent of the gap equals the width of a full-grown granule. Thus, actual 3D scattering smoothens the granular scene in the radiation impinging from below on the chromosphere.

H α CLOUD MODELING

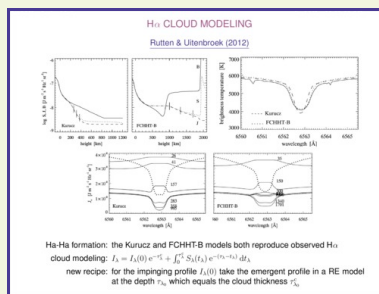
Rutten & Uitenbroek (2012)



Ha-Ha formation: the Kurucz and FCHHT-B models both reproduce observed H α

cloud modeling: $I_\lambda = I_\lambda(0) e^{-\tau_\lambda^c} + \int_0^{\tau_\lambda^c} S_\lambda(t_\lambda) e^{-(\tau_\lambda - t_\lambda)} dt_\lambda$

new recipe: for the impinging profile $I_\lambda(0)$ take the emergent profile in a RE model at the depth τ_{λ_0} which equals the cloud thickness $\tau_{\lambda_0}^c$



First row: comparison of $H\alpha$ formation in the radiative-equilibrium model without chromosphere of [Kurucz \(1992\)](#) and in the FCHHT-B model. Both have similar outward scattering declines for $H\alpha$ $S \approx J$, but located in the photosphere for the Kurucz model, in the chromosphere for the FCHHT-B model. The predicted emergent $H\alpha$ profiles are similar and reproduce the solar atlas profile fairly well.

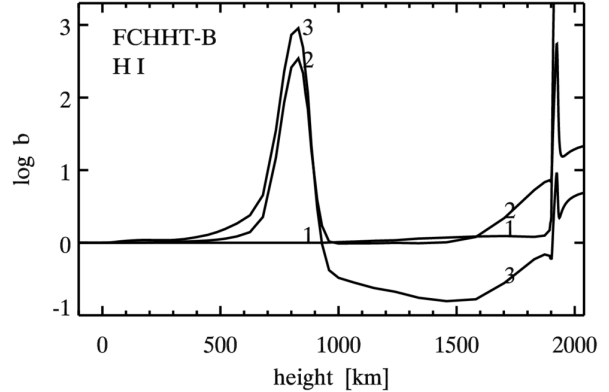
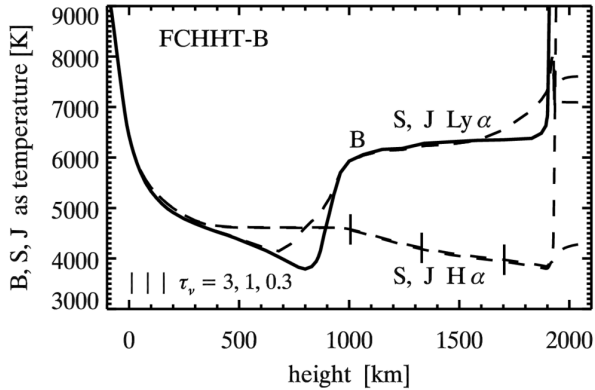
This comparison illustrates the large effect of $H\alpha$ backscattering by the FCHHT-B chromosphere. Without it $J(H\alpha)$ would drop as steeply as in the Kurucz model.

The second row compares J_{λ} profiles at various heights. They are similar in the two photospheres but of course differ higher up. The dotted curves are the radial-intensity $H\alpha$ profiles at $h = 850$ km in the FCHHT-B model and at $h = 252$ km in the Kurucz model. The line-center optical depths are $\tau_0 = 3.5$ at both locations, equalling the optical thickness of the FCHHT-B chromosphere.

The $H\alpha$ formation with an underlying opacity gap suggests cloud modeling, preferably with depth-dependent scattering S within the cloud. The suggested recipe addresses the long-standing problem of what to assume for the impinging $H\alpha$ background profile $I_{\nu}(0)$. The near equality of the dotted profiles in the second row implies that one should take the outward-intensity profile in the radiative-equilibrium model at optical depth equal to the cloud's thickness (a cloud parameter) to represent the backscattering-boosted intensity profile that impinges on the chromospheric cloud.

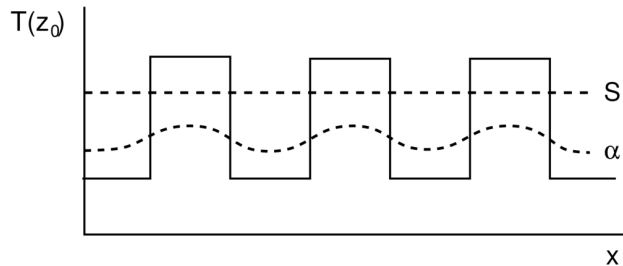
H α SMOOTHING

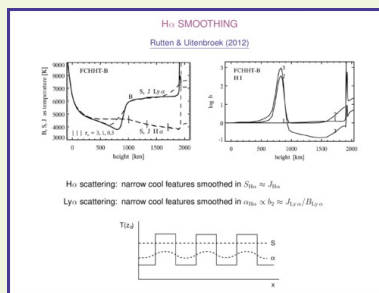
Rutten & Uitenbroek (2012)



H α scattering: narrow cool features smoothed in $S_{H\alpha} \approx J_{H\alpha}$

Ly α scattering: narrow cool features smoothed in $\alpha_{H\alpha} \propto b_2 \approx J_{Ly\alpha} / B_{Ly\alpha}$



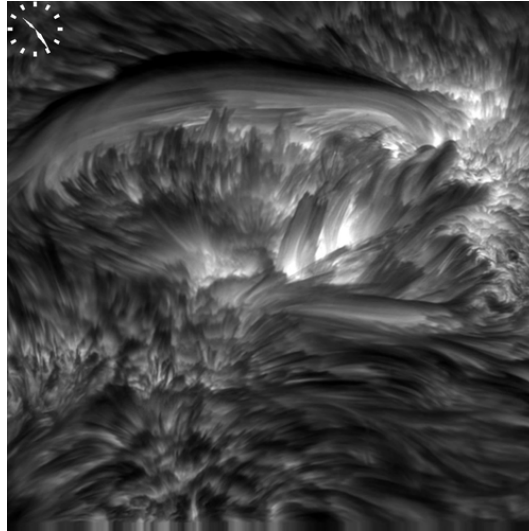


More $H\alpha$ properties illustrated with the FCHHT-B model. In 1D $H\alpha$ NLTE-scatters across its marked temperature minimum, and so does $Ly\alpha$. This is shown in the first graph plotting B , S , J for the two lines in the form of equivalent temperatures (electron, excitation, radiation) to make them comparable without difference from Planck function temperature sensitivity. The FCHHT-B chromosphere has $H\alpha$ line-center optical thickness 3.5 and mean free photon path 100 km (underneath it is as wide as the opacity gap). In $Ly\alpha$ the chromosphere thickness is 10^8 with mean free path only 1 cm at its bottom, yet smaller below. Nevertheless, $Ly\alpha$ scattering smoothens the deep source function dip that LTE would predict in the temperature minimum.

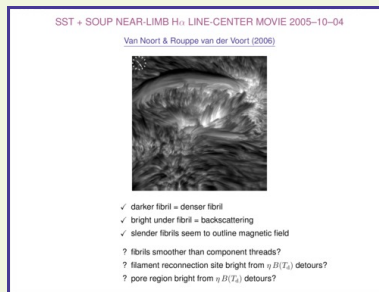
The $Ly\alpha$ scattering causes a high peak in the population departure coefficient $b \equiv n/n^{\text{LTE}}$ for level $n=2$ (lefthand graph) since $b_2 \approx b_1 (S_{Ly\alpha}/B_{Ly\alpha}) \approx J_{Ly\alpha}/B_{Ly\alpha}$ with $b_1 \approx 1$. This overpopulation of the lower level of $H\alpha$ causes a partial fill-in of the opacity gap for this line. (In the opacity plot on [this earlier display](#) the overpopulation produces the difference between the dash-dotted line-center opacity curve for LTE and the solid curve for NLTE.)

In 3D we may regard this smoothing of the deep temperature minimum and steep chromospheric temperature rise of the FCHHT-B model as indicative of what happens generally for small-scale temperature inhomogeneity, also for lateral variations. See the cartoon. The $H\alpha$ source function gets smoothed by resonance scattering in the line itself, the $H\alpha$ opacity by scattering in $Ly\alpha$.

Van Noort & Rouppe van der Voort (2006)



- ✓ darker fibril = denser fibril
- ✓ bright under fibril = backscattering
- ✓ slender fibrils seem to outline magnetic field
- ? fibrils smoother than component threads?
- ? filament reconnection site bright from $\eta B(T_d)$ detours?
- ? pore region bright from $\eta B(T_d)$ detours?

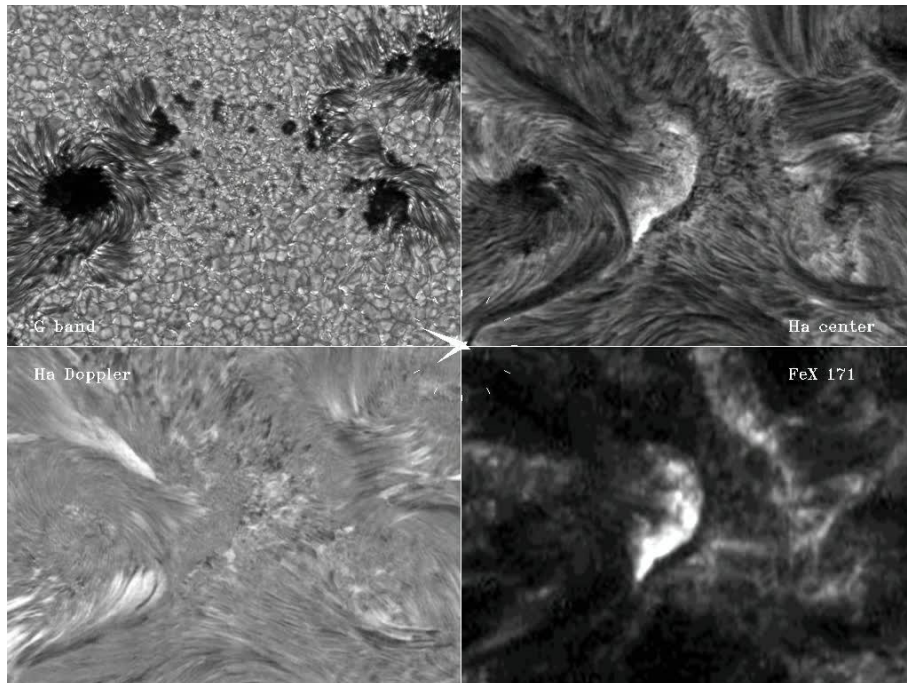


Clicking on the image in the previous display gets you a fabulous SST movie. The view is off-center ($\mu \approx 0.2$, limb towards the top) so that many structures are seen from aside. There is a decaying active region hidden under the $H\alpha$ junk, with a large pore shooting off a dark filamentary surge. DOT image sequences of the same region in multiple diagnostics are available [here](#). There are many dynamic fibrils (see [De Pontieu et al. 2007](#) who used another SST data set from the same day) visible as dark, upright, extending and retracting fingers. The small bright fast-moving features in the active-region filament are described by [Lin et al. \(2012\)](#).

Watching the long, more or less horizontal fibrils in the lower-right quadrant confirms some of my $H\alpha$ formation points. Darker fibrils indeed seem denser, with the darkest parts reaching the highest. Underneath some of the long fibrils one sees brightness that may well correspond to a backscattering-filled cool opacity void, not to hotter gas. The fibril pattern strongly suggests magnetic field topography mapping (as the dynamic fibrils indeed do, delineating wave-guided shocks).

Speculations concerning $H\alpha$ formation: the long fibrils may appear smoother than the actual thermodynamic topography due to S and τ smoothing by scattering. The sudden brightness enhancement under the filament, suggesting reconnection, may represent large detour contribution to S . The same for the bright area near the center above the large pore. Such detour photon production may come from hydrogen recombination in low-lying, unusually dense transition region gas.

DOT DISK-CENTER ACTIVE REGION MOVIE 2005-07-09



[line-center movie enlarged](#)

- ? small Doppler = hot?
- ? moss bright from $\eta B(T_d)$ detours?
- ? reconnection fronts bright from $\eta B(T_d)$ detours?



The image in the previous display opens a four-panel movie combining [DOT](#) G band, $H\alpha$ line-center and $H\alpha$ Dopplergrams with [TRACE](#) 171 Å, aligned by Alfred de Wijn. (The bright 171 Å markers identify particle hits.) The clicker underneath opens the $H\alpha$ line-center panel full-screen. The moat flow in this region was studied from simultaneous SST data by [Vargas Domínguez et al. \(2007\)](#).

There is much to see. Long fibrils at bottom center. Dynamic fibrils at top center, with dark tops extending and contracting to mask bright mossy plage. The very bright mossy area left of center, bright in both $H\alpha$ and 171 Å, has a sharp boundary to the right. The line-center enlargement movie shows sharp spreading arcs of enhanced brightness within it that smack of reconnection.

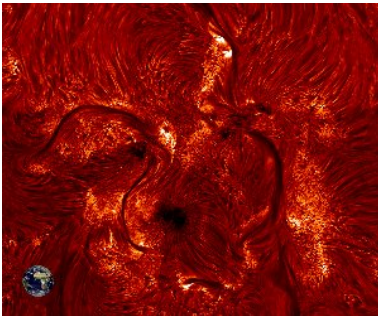
The Dopplergram signal is small in the bright mossy areas. Spreading penumbral waves are seen around every sunspot. Both the long fibrils and the short dynamic fibrils display rapidly changing black-and-white Doppler patterns.

Speculations concerning $H\alpha$ formation: the bright regions suggest fields that are more vertical, hence more interesting, than in the dynamic and long fibrils. The small Dopplergram amplitude there may be due to large thermal broadening. The $H\alpha$ and 171 Å similarity suggest $H\alpha$ brightness from $\eta B(T_a)$ detour contributions in dense low-lying transition-region gas, in agreement with the striking small-scale down-the-throat-bright patchiness of active regions in [these Ly \$\alpha\$ images](#) from the [VAULT-2 flight](#).

CONCLUSION



- *H α formation*
 - H α is a scattering line with an opacity gap
 - core darkness \sim density; core width \sim temperature
 - enhanced brightness from $\eta B(T_d)$ detours?
- *H α utilization*
 - H α fibrils chart azimuthal field component
 - use as lower boundary in NLFFF extrapolation?
 - predict free energy loading in active regions?
- *H α observation*
 - [DOT](#) H α mosaics: $3' \times 3'$ @ $0.3''$ every 3 min [$r_0 > 8$ cm]
 - no [Dutch solar physics](#) = no support anymore
 - unmothball to co-point with IRIS during 2013 and 2014?



CONCLUSION




- $H\alpha$ formation
 - $H\alpha$ is a scattering line with an opacity gap
 - core darkness ~ density; core width ~ temperature
 - enhanced brightness from $\nu_B(T_{\text{ex}})$ detours?
- $H\alpha$ utilization
 - $H\alpha$ fibrils chart azimuthal field component
 - use as lower boundary in NLFFF extrapolation?
 - predict free energy loading in active regions?
- $H\alpha$ observation
 - DOT $H\alpha$ mosaics: $\approx 1''$ @ $0.3''$ every 3 min [$\nu_B > 5$ cm]
 - no Dutch solar physics = no support anymore
 - unmothball to co-point with IRIS during 2013 and 2014?

$H\alpha$ formation: in long dark fibrils and in dynamic fibrils $H\alpha$ has Eddington-Barbier core sampling of the outward source function decline characteristic for a scattering atmosphere or slab. The emergent intensity is lower at larger density and further-out sampling. Temperature affects the core width more than the core depth. The classic “photoelectric” detour-path domination of [Thomas \(1957\)](#) may cause enhanced brightness where a dense low-lying transition region provides hydrogen recombination.

$H\alpha$ utilization: dark $H\alpha$ fibrils outline the azimuthal field component that should be valuable input to NLFFF extrapolation of active-region field topography which may lead to reliable energy-loading predictions. Vertical field features, as the RBE on-disk counterparts to spicules-II of [Roupe van der Voort et al. \(2009\)](#), are of more interest re direct upward mass, energy and helicity transfer but are harder to observe.

$H\alpha$ observation: the [DOT \(photo\)](#) remains unique in its capability to provide large-field $H\alpha$ image mosaics at $0.3''$ resolution ([example](#)) when the La Palma seeing is good. Unfortunately, its funding is gone; worse, with [Utrecht astronomy Dutch solar physics](#) is [gone](#). We would like to unmothball the DOT next year to have it co-point with [IRIS](#) to provide $H\alpha$ mosaics covering the IRIS slit wherever it is. It seems highly worthwhile to image the chromosphere around the IRIS slit. You are welcome to help achieve this goal.

DUTCH OPEN TELESCOPE

<http://www.staff.science.uu.nl/~ruttel101/dot>

*designed, built, operated by Robert H. Hammerschlag
non-vacuum inspirer for solar telescope technology*



- *properties*
 - wind-swept ocean site [south of jet streams]
 - wind-flushed but stable open tower and telescope
 - on-site cluster for speckle reconstruction
- *synchronous movie maker since 1999*
 - continua, G band, tunable Ca II H, profile-sampling $H\alpha$
 - $0.2'' - 0.3''$ resolution when $r_0 > 8$ cm
 - (pm: 80 mÅ Lyot filter for Ba II 4554 Doppler & Stokes)
- *Utrecht University saga*
 - 2003: UU evaluation “DOT pearl in crown of sciences”
 - 2007: UU ends DOT funding
 - 2008 – 2010: DOT operation on EC and NSF funding
 - 2011: UU ends Utrecht astronomy; DOT mothballed
 - 2013: $H\alpha$ mosaic sequences co-pointed with IRIS?

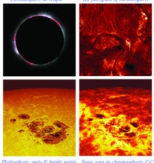


“Sol Iustitiae Illustra Nos”

- past
 - spectral line formation (1920 – 2011)
Julius, Minnaert, Houtgast, de Jager, Zwaan, Rutten
 - MHD and plasma physics (1960 – 2000)
de Jager, Kuperus, Rosenberg, Kuijpers
 - solar and stellar magnetism (1970 – 1995)
*Zwaan, Spruit, van Ballegoijen, Schrijver, Rutten**
- 2011 = the final year
 - spectropolarimetry (SOLIS, Hinode, DST/IBIS, S5T)
Keller, Snik, Fischer, Gorobets
 - photospheric & chromospheric dynamics
Leenaarts, [Vögler], [Rutten]
 - [Dutch Open Telescope](#), EST design
[Hammerschlag],[Bettonvil]
- ex-Utrecht solar physicists abroad
Henk Spruit, Aad van Ballegoijen, Piet Martens, Karel Schrijver, Paul Hick, Han Uitenbroek, Jo Bruls, Martin Volwerk, Kostas Tziotziou, Luc Rouppe van der Voort, Michiel van Noort, Alfred de Wijn, Jorrit Leenaarts, Nikola Vitas, Catherine Fischer, Gregal Vissers, Tijmen van Wettum

UNDERSTANDING AND OBSERVING THE H α CHROMOSPHERE

Rob Rutten
 Utrecht Astrophysics & Institut for Terrestrial Astrophys. Oslo
<http://www.staff.uu.se/~rstr101@astrof.uu.se>
<http://www.staff.uu.se/~rstr101@astrof.uu.se>

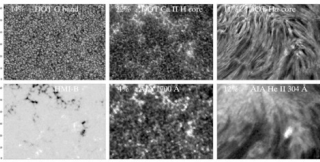


Lockyer (1866): chromosphere = off-bell emission H I Balmer + He I δ + Bal I

1

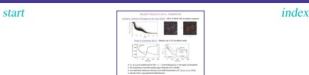
DOT & SDO IMAGE COMPARISON

Rutten & Uitenbroek (2012)



- DOT Call H & SDO 1700 Å: NW strong vertical fields; IN shocks ("clapotisms")
- DOT He: NW bright; IN fibril chromosphere
- SDO He 304 Å: NW magnetic-action bright; IN = fibril chromosphere

4



These two papers are complementary. Leenaarts et al. (2012) analyze H α formation in a snapshot from a 3D time-dependent MHD simulation (including non-equilibrium hydrogen ionization) with the *Bifrost* code. Rutten & Uitenbroek (2012) analyze H α formation in the most recent 1D static plane-parallel hydrostatic-equilibrium standard model, FCIBT-B of Fontana et al. (2009).

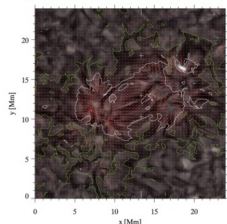
The key result is that H α is a resonant scattering line. Its line source function S is given as the angular mean of the radiation field J everywhere above the deep photosphere. There is a high- J plasma across the cool upper photosphere fed by scattering from below and from above. It is due to low line opacity as shown by the last graph for line-center and near-wing wavelengths. The optical depth buildup (indicated in negligible across this opacity gap. Above $z \approx 2$ km an extended deep slab in the σ_0 dip is a scattering isothermal atmosphere, with Edlén-Burton emergent-intensity sampling. Large thermal broadening makes the core with a temperature diagnostic (Caizzi et al. 2009).

The first image thumbnail is a clicking option the next page, showing a cutout of the *Bifrost* image when the H α formation is computed along columns in 1D fashion. The next page has this done in 3D. Think the two to see how striking the fibril core into view in the 3D case. The underlying larger-contrast granulation pattern is washed out by J -scattering across the opacity gap.

The second image thumbnail opens a page with figure 13 of Leenaarts et al. (2012). Blow it up to convince yourself that the fibril roughly outline the simulated field direction (red arrows).

7

Figure 13 Leenaarts, Carlsson & Rouppie van der Voort (2012) index



10

start index



Format: in this workshop Jakob used pages after each talk display that contain my oral explanation (or rather, what I wanted to say but didn't have the time limit). I replaced mouse-opening clickers by weblinks to download them, and turned citations into weblinks that should open the corresponding ADS page in your browser.

Navigation: clicking on the display title or thumbnail returns you to where you came from. Each talk display also has a hidden clicker top-left returning you to the first display, and one at top-right to a thumbnail table. These are explicit in the linked inset pages, as here.

Title: this talk is mostly about understanding the formation of H α , with a plea for He I for observing for IRIS at the end.

My affiliation: I spent fifty years in solar physics at Uppsala, but since early 2012 I teach astronomy in *pace*. Dutch solar physics vanished with it. Finally, I am still welcome at OSO.

Graphical introduction to NLF chromospheric line formation: a similarly expanded portion of a 3D numerical core of the SDO-IRIS/Hinode Wind-up and Memory archive this year. It covers the same He I results but adds an extended diagnostic scattering in the solar atmosphere.

2

start index



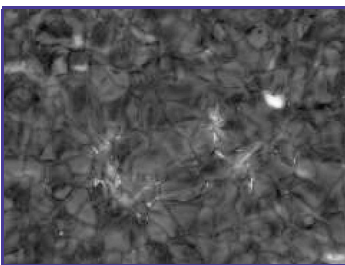
A more detailed scene comparison for an area with plage (upper part of the field of view) and quiet network and internetwork (lower part). Upper row: images from the DOT. Lower row: images from SDO. The percentage numbers specify the relative rms brightness contrast per image. Solar images are usually byte-scaled for maximum display contrast; the actual contrast is often much lower.

First column: photosphere. The principal ingredients are the granulation and strong-field magnetic concentrations, with μ -mode evolution evident in time-sequence sampling. Zooming in on the G-band bright points shows their close correspondence with (unpolarized) IMF field concentrations.

Second column: bright chromosphere in plage and network but shock-aided narrow "clapotisms" elsewhere. The latter gaps, underneath the H α fibrils, not chromosphere because it does not radiate H α . The Ca II H and I 854 Å scenes are closely similar, apart from obvious differences in sharpness. The rms contrast differs much because such wide-band Ca II H is dominated by near-LTE inner-wing brightness. I 854 Å by band-core scattering.

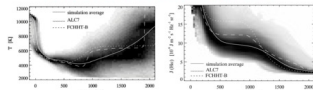
Third column: chromosphere. Both H α and He II 304 Å show bright grains at fibril footpoints near magnetic concentrations and darker fibrils covering the internetwork, with some but not 1:1 similarity between the two diagnostics. He II 304 Å is supposed to sample the transition region. The rough similarity suggests that the latter shares the fibrillar morphology of the chromosphere. However, the bright blob seems specific for He II 304 Å.

5



8

OSLO SIMULATION VERSUS 1D STANDARD MODELS



- simulation = state of the art: 3D(0), β_0 non-He, SE populations but NE for H (Leenaarts, Carlsson & Rouppie van der Voort (2012))
- ALC7 = UV fit: 1D static, no β_0 , He I microturbulence, SE populations (Auréli & Lousier (2008))
- FCIBT-B = UV fit: 1D static, no β_0 , He I imposed acceleration, SE populations (Fontana, Guizi, Hamelin, Harder & Tuin (2009))

11

start index



The above image quartet mirrored the decadal survey White Paper by *Sten et al.* (2009). The first image illustrates the naming of the chromosphere by Lockyer (1866) (I typed the report into ADS). Using a new spectroscopy he found a pink ring around the Sun, also outside prominences, dominated by a few Fraunhofer lines later identified as H α , He I δ , He II, and Bal I. By definition the chromosphere is whatever emits these lines, making H α the quintessential chromospheric diagnostic. Cf H&A&A column eleven.

The second image, from the DOT, shows the H α chromosphere on the disk. It is a dense mass of fibrils wherever there is a bit of activity. It is not clear whether these fibrils are cylindrical filaments, edge-on (or = coronations, shears, or sheet waves) receding/corotating fields. They seem to outline horizontal field topology. Vertical fields are less easily seen in He I but are of larger interest to coronal mass and energy budget (see Rutten 2012 for an overview).

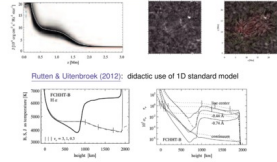
The lower-left DOT image shows the photosphere in the G-band. Its bright points mark strong-field footpoints, without sign. Signal magnetograms from MDI and HMI are habitually used for field topology mapping. Since it becomes finer-and-finer as close to the chromosphere, He fibril patterns cannot be produced this way. They are best monitored SDO-like and contrast NIFF extrapolation.

The lower-right DOT image is corresponding wide-band Ca II H. It shows chromospheric emission where it is bright, elsewhere cool shock ridges gap underneath the fibril chromosphere.

3

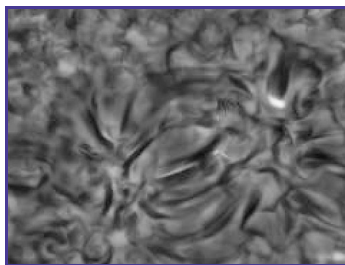
RECENT RESULTS ON H α FORMATION

Leenaarts, Carlsson & Rouppie van der Voort (2012): 3D(0)-R-MHD-NE simulation snapshot



- H α is a pure scattering line with $S = J$ and small opacity in the upper photosphere
- 3D scattering across the opacity gap enhances fibril visibility
- core darkness measures density, core width temperature (cf. Caizzi et al. 2009)
- slender fibrils may accumulate field direction

6



9

start index



Comparison between the Oslo Bifrost simulation and the latest 1D standard models. The gray-scale measures the occurrence probability per pixel across the simulation as plotted at the given height. Left: temperature against height. Right: mean intensity J at He I line-center against height.

The refraction in simulation temperature at the deeper layers separates granules and intergranular lanes. The narrow neck in the upper photosphere temperature, above chromospheric granulation and below the growth of acoustic waves into shocks, is close to 1D radiative-equilibrium models. However, the spread in J (He I) is already large.

The FCIBT-B chromosphere, supported by ad-hoc postulated equilibrium, has isothermal-slab character. The deep temperature minimum below it boosts J across the corresponding H α opacity gap by strong back-scattering from the slab. Higher up, the constant $J = J$ scattering slab of He I is similar for the three curves.

The J and J (He I) behaviors may seem equally similar between the simulation and standard models. However, the conceptual differences between plane-parallel static hydrostatic-equilibrium modeling and the 3D(0) MHD simulation are enormous (cf. Neoviuson gravitation versus general relativity). The J (He I) stratifications in the simulation vary tremendously, with shocks propagating upwards and sideways along fields and the increase to coronal temperature during opacity up and down over a large height range. The standard models cannot be taken as a quiet-temperature of these variations.

12

13

CANONICAL CHROMOSPHERIC LINE FORMATION

• CRD line source function including detour paths:

$$S_i^* = \frac{2n_i + c_i R_i(T_i) + c_i' R_i(T_i)}{1 + c_i R_i(T_i) + c_i' R_i(T_i)}$$

$$= \frac{1 - c_i' + c_i R_i(T_i) + c_i' R_i(T_i)}{1 + c_i R_i(T_i) + c_i' R_i(T_i)}$$

- $c_i =$ upper-lower collisional destruction fraction of total extinction
- $c_i' =$ detour-path extinction fraction of total extinction
- $c_i' / c_i =$ detour path ratio to scattering extinction
- $T_i =$ profile-averaged angle-integrated intensity
- $T_i =$ formal detour extinction temperature: $(n_i D_{ul} / (g_i D_{ul})) \approx \exp(h_i / T_i)$
- line source function S_i^* (Thomas 1997)
- "coolion type" (H & K) or "gristichion type" (H_{α} , Balmer continuum leading)

14

start **index**

Canonical wisdom: The graphs show the Planck function B and line source function S^* against optical depth (outward to the left). Both graphs are reprinted in both the first (1970) and second (1976) editions of Milne's "Stellar Atmospheres". Jefferts & Thomas (1959) produced them to illustrate the classification of Thomas (1957), yielding lines between "coolion type" at left and "gristichion type" at right. They named Ca II H & K as example of the first. *Ho* is an example of the latter.

The difference was assigned to the τ_{10} ratio. For H_{α} the high source function across the upper photosphere is the right-hand graph and attributed to preponderance of detour path (c_i' / c_i) contribution. For H_{β} typically Balmer photoionization up from $\tau = 2$ plus cascade recombination (into high τ followed by downward $\Delta\tau = 1$ steps) down to emission.

The various curves in the left-hand graph show the source functions of Na I D₁, Ca II 8542 Å, Ca II K, and Mg II λ with c_i and c_i' as indicated. Note that for H_{α} the simulation employed an ad hoc standard model in a scattering-dominated line gas yet also, with negligible detour contribution except in the transition region. Its unusual superheated upper-photosphere source function comes instead from chromospheric backscattering across its unusual opacity gap.

15

H α SOURCE FUNCTION IN THE FCHFB-B MODEL

Rutten & Uitenbroek (2012)

- $S_i^* = \frac{1 - (1 - c_i) \tau_{10} - c_i' R_i(T_i) + c_i R_i(T_i) + c_i' R_i(T_i)}{1 + c_i R_i(T_i) + c_i' R_i(T_i)}$
- The detour part $\frac{c_i' R_i(T_i)}{1 + c_i R_i(T_i) + c_i' R_i(T_i)}$ exceeds the collision part $\frac{c_i R_i(T_i)}{1 + c_i R_i(T_i) + c_i' R_i(T_i)}$. However, their sum $\frac{c_i R_i(T_i) + c_i' R_i(T_i)}{1 + c_i R_i(T_i) + c_i' R_i(T_i)}$ (bold) reaches only a few percent to $S_i \approx J_{\nu}$.
- The H_{α} core is dominated by resonance scattering with a formation gap below the chromosphere filled by backscattered radiation. The FCHFB-B chromosphere acts as scattering attenuator building up its own irradiation. Most emerging photons are created in the deep photosphere where $c_i \approx 1$ and $J_{\nu} \approx B_{\nu}(T_i)$.
- The FCHFB-B H_{α} core profile is well described by the Eddington-Barbier approximation for an irradiated line isothermal scattering atmosphere.

16

start **index**

H α formation in the FCHFB-B model. This model is suitable to describe any actual column in the solar atmosphere over a quasi-thermal-optical range, but it serves here for didactic breakdown.

Left: H_{α} S_i^* with $S_i^* \approx S^*$ (thin solid) and $J_{\nu} \approx J$ (dashed). Note that everywhere below the transition in the corona $S_i^* > J_{\nu}$, in particular at $\tau = 0.5 - 1$ (formation stage).

Right: fluxion collisional (dashed) and detour (dash-dotted) contributions to S_i^* as specified under the first bullet. The detour becomes dominant in the transition in the corona, but that is intransparent. Elsewhere $S_i^* > J_{\nu}$. Thus, it is a scattering line. H_{α} photons created in the deep chromosphere. Backscattering across the temperature-minimum opacity gap holds us J_{ν} there.

Dimming the FCHFB-B chromospheric temperature produces appreciably higher $S_i^* \approx J_{\nu}$, peaking at 6000 K just above the gap, but also lower H_{α} fluxion intensity at 1700 km. This further-out sampling of the outward J_{ν} decline compensates for the increase, so that $(J_{\nu} / S_i^*) \approx 1$ remains nearly the same. Dimming the chromospheric density produces only 200 K higher J_{ν} across the gap, less downward, but also moves $\tau = 1$ to about 1700 km and lowers the emergent core intensity appreciably. The core intensity is a density rather than a temperature diagnostic.

The height extent of the gap equals the width of a full-grown granule. Thus, actual ID scattering encompasses the granular scale in the radiation impinging from below on the chromosphere.

17

H α CLOUD MODELING

Rutten & Uitenbroek (2012)

H α formation: the Kurucz and FCHFB-B models both reproduce observed H α cloud modeling, also for lateral variations. See the curves. The H α source function gets new recipe: for the impinging profile $J_{\nu}(0)$ take the emergent profile in a RE model in the depth τ_{10} , which equals the cloud thickness τ_{10} .

18

start **index**

First row: comparison of H_{α} formation in the radiative-equilibrium model without chromosphere of Kurucz (1992) and in the FCHFB-B model. Both have similar outward decline for H_{α} S_i^* J_{ν} . But located in the photosphere for the Kurucz model, in the chromosphere for the FCHFB-B model. The predicted emergent H_{α} profiles are similar and reproduce the solar atlas profile fairly well. This comparison illustrates the large effect of H α backscattering by the FCHFB-B chromosphere. Without it Kurucz would dip steeply in the Kurucz model.

The second row compares J_{ν} profiles at various heights. They are similar in the two photospheres but of course differ higher up. The actual curves are the radial intensity H_{α} profiles at $r = 850$ km of the FCHFB-B model at $\tau = 252$ km in the Kurucz model. The center optical depth are $\tau_{10} \approx 1.5$ at both locations, equalling the optical thickness of the chromosphere.

The H_{α} formation with an underlying opacity gap suggests cloud modeling, preferably with depth-dependent scattering S_i^* within the cloud. The suggested recipe is the long-standing problem of what to assume for the impinging H_{α} cloud profile $J_{\nu}(0)$. The equality of the defined profiles in the second row implies that one should take the outward-intensity profile in the radiative-equilibrium model at optical depth equal to the cloud's thickness in cloud parameter to reproduce the backscattering-biased intensity profile that impinges on the chromosphere.

19

H α SMOOTHING

Rutten & Uitenbroek (2012)

H α scattering: narrow cool features smoothed in $S_{H\alpha} \approx J_{\nu}$.

L γ scattering: narrow cool features smoothed in $S_{L\gamma} \approx J_{\nu} + J_{L\gamma} \tau_{10}$.

20

start **index**

More H_{α} properties illustrated with the FCHFB-B model. In ID H_{α} NEZC-scatters across its marked temperature minimum, and so does L γ . This is shown in the first graph plotting S_i^*, J_{ν} for the rest lines in the form of equivalent temperature (electron, excitation, radiation) to make them comparable without difference from Planck function temperature sensitivity. The FCHFB-B chromosphere has H_{α} fine-center optical thickness 1.5 and mean free photon path 100 km (underneath it is as wide as the opacity gap). In L γ the chromospheric thickness is 10 τ_{10} with mean free path only 1 cm at the bottom, yet smaller below. Nevertheless, L γ scattering smoothes the deep source function dip that LTE would predict in the temperature minimum.

The L γ scattering causes a high peak in the population amplification coefficient $b_{\nu} = n_{\nu} / n_{\nu}^{(0)}$ for level $n = 2$ (different graph) since $b_{\nu} = b_{\nu}(S_{\nu} / B_{\nu}) \approx J_{\nu} / B_{\nu} \approx J_{\nu} / \tau_{10}$ with $b_{\nu} \approx 1$. This overpopulation of the lower level of H_{α} causes a partial flip of the opacity gap for the line. In the opacity gap on this center dip the overpopulation produces the difference between the dash-dotted line-center opacity curve for L γ and the solid curve for NEZC.

In 3D we may regard this smoothening of the deep temperature minimum and steep chromospheric temperature rise of the FCHFB-B model as indicative of what happens generally for small-scale temperature inhomogeneity, also for lateral variations. See the curves. The H α source function gets smoothed by resonance scattering in the line itself, the H α opacity by scattering in L γ .

21

SST + SOUP NEAR-LIMB H α LINE-CENTER MOVIE 2005-10-04

Van Noort & Rouppen van der Voort (2006)

- darker fibril = denser fibril
- brighter/darker = backscattering
- slender fibrils seem to outline magnetic field
- fibrils smoother than component threads?
- filament reconnection site bright from η (EUV) detours?
- pore region bright from η (EUV) detours?

22

start **index**

Clicking on the image in the previous display gets you a 640x480 SST movie. The view is off-center ($\mu = 0.2$, limb towards the top) so that many structures are seen from above. There is a deep jet active region hidden under the H_{α} jet, with a large pore showing off a dark filamentary source. DOT image sequence of the same region in multiple diagnostics are available here. There are many dynamic fibrils (see De Pontieu et al. 2007 who used another SST data set from the same day) visible as dark, wiggly, extending and retracting fingers. The small bright fine-moving features in the active region filament are described by (van der Voort 2012).

Watching the long, more or less horizontal fibrils in the lower-right quadrant confirms some of my H_{α} formation points. Darker fibrils indeed seem denser, with the darker parts reaching the highest. Underneath some of the long fibrils one sees brightness that may well correspond to a backscattering-filled cool opacity void, not to hotter gas. The third parameter strongly suggests magnetic field topology mapping (in the dynamic fibrils or ad, delineating wave-guided shocks).

Speculations concerning H_{α} formation: the long fibrils may appear smoother than the actual thermodynamic opacity due to S_i^* smoothing by scattering. The wider brightness enhancement under the filament, suggesting inhomogeneity, may represent large dark-arc contribution to S_i^* . The same for the bright area near the center above the large pore. Such denser photos production may come from hydrogen recombination in low- τ , unusually dense transition region.

23

DOT DISK-CENTER ACTIVE REGION MOVIE 2005-07-09

Line-center opacity elongation

- small doppler + hot?
- more bright from η (EUV) detours?
- reconnection fronts bright from η (EUV) detours?

24

start **index**

The image in the previous display gets a four-panel movie combining DOT G band, He line-center and H_{α} Dopplegrams with TRACE 171 Å, aligned by Alfred de Witte. The bright 171 Å features identify particle hits. The clicker underneath opens the He line-center panel full-screen. The movie in this region was studied from simultaneous SST data by Szepes (University of Ljubljana, 2007).

There is much to see. Long fibrils at bottom center. Dynamic fibrils at top center, with dark spots extending and contracting to make bright regions. The very bright narrow area left of center, bright in both He and 171 Å, has a sharp boundary on the right. The line-center elongation shows sharp spreading area of enhanced brightness within that stack of reconnection.

The Dopplegram signal is small in the bright narrow areas. Spreading geometrical sources seem around every sample. Both the long fibrils and the short dynamic fibrils display rapidly changing Mack and white Doppler patterns.

Speculations concerning H_{α} formation: the bright regions suggest fields that are more vertical, hence more interesting, than in the dynamic and long fibrils. The small Dopplegram amplitude there may be due to large thermal broadening. The He I and 171 Å similarly suggest its brightness from $[T_e]$ detour contributions in dense low-lying transition region gas, in agreement with the striking small-scale down-the-three-bright-patches-of-active-regions in these L γ images from the VALLET-Flight.

25

CONCLUSION



- H α formation**
 - H α is a scattering line with an opacity gap
 - core darkness - density; core width - temperature
 - enhanced brightness from $\omega(H\alpha)$ detours?
- H α utilization**
 - H α fibrils chart azimuthal field component
 - use as lower boundary in NLFFF extrapolation?
 - predict free energy loading in active regions?
- H α observation**
 - DOT H α mosaics: $7 \times 7 @ 0.3''$ every 3 min [$\lambda > 1 \text{ cm}$]
 - no Dutch solar physics - no support anymore
 - unmottal to co-punt with IRIS during 2013 and 2014?



26

start **index**



H α formation: in long dark fibrils and in dynamic fibrils H α . An Edgington-Barber core sampling of the outward source function decline characteristic for a scattering atmosphere or slab. The emergent intensity is lower at larger density and further out sampling. Temperature affects the core width more than the core depth. The classic "phenomenon": Active-pole domination of *Thomas (2007)* may cause enhanced brightness where a dense low-lying transition region provides hydrogen recombination.

H α utilization: dot H α fibrils outline the azimuthal field component that should be suitable input to NLFFF extrapolation of active-region field topology which may lead to reliable energy-loading predictions. Vertical field features, as the *RBE* on-disk counterparts in spicules II of *Isopope van der Horst et al. (2009)*, are of more interest to direct upward mass, energy and helicity transfer but are harder to observe.

H α observation: the DOT (photo) remains unique in its capability to provide large-field H α image mosaics at 0.3'' resolution (example) when the La Palma seeing is good. Unfortunately, its finding is gone: worse, with Utrecht astronomy Dutch solar physics is gone. We would like to unsmother the DOT next year to have it co-punt with IRIS to provide H α mosaics covering the RES etc whenever it is. It seems highly worthwhile to image the chromosphere around the RES etc. You are welcome to help achieve this goal.

27

DUTCH OPEN TELESCOPE

<http://www.staff.science.uu.nl/~dutsr001/gos>
 designed, built, operated by Robert H. Hammerschlag
 non-vacuum inspired for solar telescope technology




- properties**
 - wind swept ocean site [south of jet streams]
 - wind flushed but stable open tower and telescope
 - on-site cluster for speckle reconstruction
- synchronous movie maker since 1989**
 - continua, G band, tunable Ca II H, profile sampling H α
 - 0.2''-0.3'' resolution when $\tau_{10} > 1 \text{ cm}$
 - (gm: 80 mA Lyot filter for Ba II 4554 Doppler & Stokes)
- Utrecht University saga**
 - 2003: UU evaluation "DOT pearl in crown of sciences"
 - 2007: UU ends DOT funding
 - 2006 - 2010: DOT operation on EG and NSF funding
 - 2011: UU ends Utrecht astronomy; DOT mottalbed
 - 2013: H α mosaic sequences co-punted with IRIS?

28

UTRECHT SOLAR PHYSICS

"Sol Justitiae Illustra Nos"



Universiteit Utrecht
Sterrekundig Instituut

- past**
 - spectral line formation (1900 - 2011)
 - Julius Minkowski, August de Jager, Zwaan, Rutten
 - MHD and plasma physics (1960 - 2000)
 - de Jager, Kuperus, Rosenberg, Kijpers
 - solar and stellar magnetism (1970 - 1995)
 - Zwaan, Spruit, van Ballegoijen, Schrijver, Rutten*
- 2011 = the final year**
 - spectropolarimetry (SOLS, Hinode, DST/IBIS, SST)
 - Keller, Sisk, Fischer, Gonzalez
 - photospheric & chromospheric dynamics
 - Leenaarts, [Vögler], [Rutten]
 - Dutch Open Telescope, EST design
 - [Hammerschlag], [Bettovivi]
- ex-Utrecht solar physicists abroad**
 - Henk Spruit, Aad van Ballegoijen, Piet Martens, Karel Schrijver, Paul Hek, Henk Ueberrode, Jo Bruls, Martin Solovik, Keesje Toizobu, Luc Rogge van der Voort, Michiel van Noord, Alfred de Wijn, Jorrit Leenaarts, Nikolai Vilas, Catherine Fischer, Gergely Vissers, Tjmen van Westrum

29



30

